

Searching for exclusive leptoquarks with the Nambu-Jona-Lasinio composite model at the LHC and HL-LHC

S. AJMAL,^{1,2} J. T. GAGLIONE,³ A. GURROLA,³ O. PANELLA,²

M. PRESILLA,⁴ F. ROMEO,³ H. SUN,⁵ and S.-S. XUE^{6,7,2,8}

¹*Dipartimento di Fisica e Geologia, Univeristà degli Studi di Perugia, Italy*

²*INFN, Sezione di Perugia, Via A. Pascoli, I-06123, Perugia, Italy*

³*Department of Physics and Astronomy, Vanderbilt University, Nashville, TN, 37235, USA*

⁴*Institute for Experimental Particle Physics (ETP), Karlsruhe Institute of Technology (KIT),
Wolfgang-Gaede-Straße 1, 76131 Karlsruhe, Germany*

⁵*Institute of Theoretical Physics, School of Physics, Dalian University of Technology,
No.2 Linggong Road, Dalian, Liaoning, 116024, P.R.China*

⁶*ICRANet, Piazzale della Repubblica, 10-65122, Pescara, Italy*

⁷*Physics Department, Sapienza University of Rome,
Piazzale Aldo Moro 5, 00185 Roma, Italy*

⁸*ICTP-AP, University of Chinese Academy of Sciences, Beijing, China*

(Dated: December 1, 2023)

We present a detailed study concerning a new physics scenario involving four fermion operators of the Nambu-Jona-Lasinio type characterized by a strong-coupling ultraviolet fixed point where composite particles are formed as bound states of elementary fermions at the scale $\Lambda = \mathcal{O}(\text{TeV})$. After implementing the model in the Universal FeynRules Output format, we focus on the phenomenology of the scalar leptoquarks at the LHC and the High-Luminosity option. Leptoquark particles have undergone extensive scrutiny in the literature and experimental searches, primarily relying on pair production and, more recently, incorporating single, t-channel, and lepton-induced processes. This study marks, for the first time, the examination of these production modes at varying jet multiplicities. Novel mechanisms emerge, enhancing the total production cross-section, especially for leptoquarks couplings to higher fermion generations. A global strategy is devised to capture all final state particles produced in association with leptoquarks or originating from their decay, which we termed “exclusive”, in an analogy to the nomenclature used in nuclear reactions. The assessment of the significance in current and future LHC runs, focusing on the case of leptoquark coupling to a muon - c quark pair, reveals superior sensitivity compared to ongoing searches. Given this heightened discovery potential, we advocate the incorporation of exclusive leptoquark searches in future investigations at the LHC.

PACS numbers: 12.60.-i,12.60.Rc,14.80.-j

CONTENTS

I. Introduction	3
II. Nambu-Jona-Lasinio composite leptoquark model	5
III. Signal implementation and samples generation	8
IV. Exclusive LQ production	9
A. Lepton initiated LQ production	12
V. Search strategy	13
VI. Expected sensitivity at LHC and HL-LHC	14
VII. Summary and remarks	16
Acknowledgments	18
References	18

I. INTRODUCTION

Thanks to its remarkably strong quantitative agreement with experimental results over the past decades, the Standard Model (SM) has been solidified as a cornerstone of elementary particle physics. Nonetheless, it is regarded as an effective theory that falls short in encompassing several foundational aspects of both theoretical and observed particle physics. Numerous extensions have been put forward, suggesting specific tests to challenge the SM at the LHC. Regrettably, all of these searches have thus far yielded a negative outcome in the quest for detecting new physics and have placed significant constraints on many beyond-the-SM (BSM) models in mass scales up to a few TeV [1–8].

Therefore, the question arises as to whether ongoing searches have exhaustively explored all avenues, or if unprecedented aspects can yet be harnessed to devise better methods that would probe yet uncharted territory. In this paper, we present an in-depth phenomenological study of a novel composite scenario based on Nambu-Jona-Lasinio (NJL) type four-fermion operators recently proposed in [9, 10]. The model is characterized by a strong coupling ultraviolet (UV) fixed point where composite particles arise as bound states of SM elementary fermions. The effective four-fermion interactions considered in this new model are motivated by theoretical inconsistencies [11–13] between the SM bilinear Lagrangian of chiral gauged fermions and the UV regularization of some unknown dynamics, such as quantum gravity. These inconsistencies imply, at high energies, quadrilinear effective operators (four-fermion interactions) of the NJL or Einstein-Cartan type [14–16]. A first phenomenological study related to the production at the LHC of composite fermions in the gauge symmetric phase of this NJL model was conducted in [17] where a recent CMS analysis [18] of the dilepton and diquark final state $pp \rightarrow \ell\ell + qq$ was recast to derive constraints on the parameter space of the NJL model. More recently a study of neutrino-less double beta decay [19] addressed the broken-gauge phase of the model. In this work we specifically address the phenomenology at the LHC of the scalar leptoquarks (LQs) arising in the gauge symmetric phase of the model, thus delving into one of the most extensively studied subjects in the BSM landscape. While reviewing current investigations, production modes, and search strategies, we investigate the potential for new mechanisms and approaches at the LHC.

LQs are hypothetical particles that carry both lepton number L and baryon number B , have a fractional electric charge, and can be either scalar (spin 0) or vector (spin 1) particles. They offer a natural explanation for the symmetry between the quark and lepton families, attempting to pave the way toward matter unification. They inherently appear in many well-motivated ex-

tensions of the SM that endeavor to unify the fundamental interactions, such as grand unified theories [20–25], technicolor models [26–29], and compositeness scenarios [30, 31], as well as R -parity violating supersymmetry [32–41], and as mediators of dark matter-SM interactions [42]. More recently, LQs have gained enhanced interest, as they provide a suitable explanation for a series of anomalies observed in several precision measurements: the $B \rightarrow D^*$ anomaly reported by BaBar [43, 44], Belle [45], and LHCb [46] that could be explained by the mediation of an intermediate LQ scalar [47–53]; the muon anomalous magnetic moment $(g - 2)_\mu$ measurement from the E989 and E821 collaborations [54, 55] which could be resolved assuming the existence of LQs [54, 56–70]; the charged proton radius obtained from muon Lamb shift [71], and atomic parity violation [72, 73], where low-energy corrections via virtual LQ scalars and internal loop diagrams can contribute. In a search for a LQ coupling to a τ lepton and a b quark, the CMS collaboration has reported an excess with a significance of 2.8 standard deviations above the SM expectation using Run 2 data [74], though consistency with the SM prediction is observed in a similar search from the ATLAS collaboration [75].

Both the ATLAS and the CMS collaborations have a broad LQ search program that covers various particle hypotheses and different lepton-quark-LQ vertex couplings λ . The main production modes considered are illustrated in Fig.1 (a - d) and have been extensively discussed in literature [53, 76–86]. The majority of the analyses rely on the LQ pair production mode in Fig.1 (c) [2, 87–120], which does not depend on λ . Some searches are designed to intercept the single LQ production process in Fig.1 (b) [75, 121–123] or the single and pair productions together [7, 75, 124], as the former brings enhanced sensitivity due to a cross-section that varies as a function of λ^2 . A recent investigation [125] added further Drell-Yan dilepton t-channel contributions as displayed in Fig.1 (a) and [126] was designed specifically for this process, whose cross-section depends on λ^4 . An additional recent search relies on lepton-induced processes [127], as that in Fig.1 (d).

Upon reviewing the existing literature and LHC searches, a noteworthy observation emerges: the generation of LQs via t-channel, single, and pair production processes is solely regarded in terms of their primary production modes. No studies have been carried out to explore the implications of these production mechanisms at various jet multiplicities, assuming that a jet is originating from either a gluon or a quark. Nevertheless, previous research [128–135] has demonstrated that such an approach could amplify the discovery potential by incorporating additional signal sources while effectively reducing the SM background. In this work, we pursue this effort and investigate how LQs would manifest in association with jets. Our investigation uncovers new production mechanisms and topological aspects not yet considered in ongoing searches. Furthermore, we devise

a comprehensive strategy to look for LQs, taking into account all signal contributions. For the case of the lepton-induced process, we undertake a study to separate elastic and inelastic contributions. Our findings reveal that the sensitivity achieved surpasses that of all ongoing searches. This new approach developed here for the specific case of LQs can be adapted and applied in searches for any type of particle to enhance further the expected sensitivity.

In Section II, we introduce the reference LQ model utilized in this analysis, while in Section III we delve into its implementation and the generation of the signal samples. Section IV describes the LQ production modes in conjunction with jets and touches upon the possibility of distinguishing elastic and inelastic lepton-induced processes. In Section V and Section VI, we present a global strategy for the detection of LQs based on our findings, as well as the anticipated sensitivity results at both the LHC and the High-Luminosity (HL)-LHC. Finally, in Section VII, we summarize the work with some closing remarks.

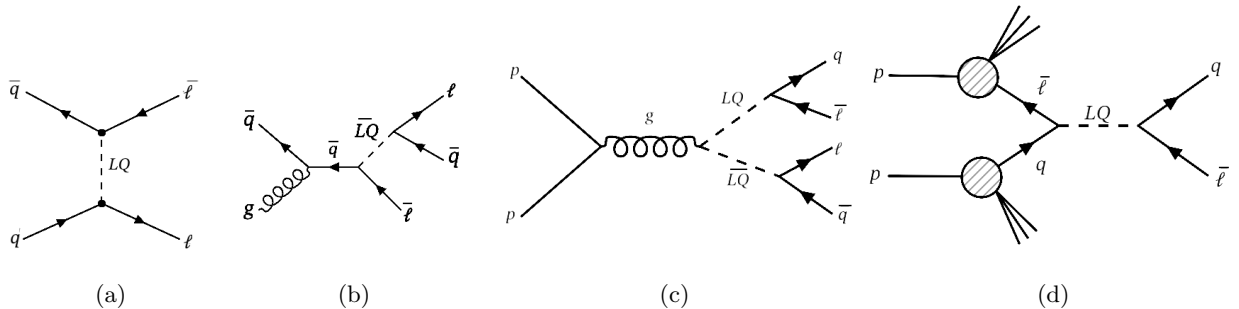


FIG. 1: Examples of Feynman diagrams for the pair (a), single (b), t-channel (c), and lepton-induced (d) production modes considered at the LHC.

II. NAMBU-JONA-LASINIO COMPOSITE LEPTOQUARK MODEL

The No-Go theorem [136, 137] shows that, as a renormalizable quantum field theory at infrared (IR) low energies, the SM *bilinear* fermion Lagrangian at UV cutoff Λ_{cut} suffers theoretical inconsistencies with SM chiral gauge symmetries and fermion spectra at low energies. This implies that new physics at the UV scale Λ_{cut} effectively presents *quadrilinear* operators $G_{\text{cut}} \bar{\psi}_L^f \psi_R^f \bar{\psi}_R^f \psi_L^f$ ($G_{\text{cut}} \propto \Lambda_{\text{cut}}^{-2}$) [9, 10] of Nambu-Jona-Lasinio (NJL) or Einstein-Cartan type. They are SM gauge symmetric interactions of SM left- and right-handed fermions (ψ_L^f, ψ_R^f) in the family “ f ”. The strong coupling $g_{\text{cut}} = G_{\text{cut}} \Lambda_{\text{cut}}^2 > 1$ dynamics leads to massive composite bosons $\Pi^f \sim (\bar{\psi}_R^f \psi_L^f)$ and fermions $F_R^f \sim \psi_R^f (\bar{\psi}_R^f \psi_L^f) \sim \psi_R^f \Pi^f$ [138–140]. They carry SM charges and couple to massless

Bosons Π_a^Q	Charge $Q_i = Y + t_{3L}^i$, $SU_L(2)$ 3-isospin t_{3L}^i , $U_Y(1)$ charge Y , $SU_c(3)$ color a ,	LQ			
$\Pi_a^{+5/3} \propto \bar{e}_R u_{La}$	+5/3	+1/2	+7/6	3	$R_2^{+5/3}$
$\Pi_a^{-1/3} \propto \bar{\nu}_R^e d_{La}$	-1/3	-1/2	+1/6	3	$\tilde{R}_2^{-1/3}$
$\Pi_{u_a}^{+2/3} \propto \bar{\nu}_R^e u_{La}$	+2/3	+1/2	+1/6	3	$\tilde{R}_2^{+2/3}$
$\Pi_{d_a}^{+2/3} \propto \bar{e}_R d_{La}$	+2/3	-1/2	+7/6	3	$R_2^{+2/3}$
$\Pi_a^{-5/3} \propto \bar{u}_R e_L$	-5/3	-1/2	-7/6	3	$R_2^{-5/3}$
$\Pi_a^{+1/3} \propto \bar{d}_R \nu_L^e$	+1/3	+1/2	-1/6	3	$\tilde{R}_2^{+1/3}$
$\Pi_{u_a}^{-2/3} \propto \bar{u}_R \nu_L^e$	-2/3	+1/2	-7/6	3	$R_2^{-2/3}$
$\Pi_{d_a}^{-2/3} \propto \bar{d}_R e_L$	-2/3	-1/2	-1/6	3	$\tilde{R}_2^{-2/3}$

TABLE I: Composite bosons, their constituents, standard model charges, and corresponding leptoquark according to the nomenclature used in [145, 146] for the first generation of standard model fermions.

SM gauge bosons in a gauge-invariant manner. The effective SM gauge symmetric and renormalizable theory realizes in the scaling domain of the UV fixed point g_{cut}^* at the composite scale $\Lambda \ll \Lambda_{\text{cut}}$ [10, 141]. As the energy scale decreases below Λ , the effective theory undergoes [142] a phase transition of composite particle decays into constituents and spontaneous SM symmetries breaking via the top-quark channel ($\bar{t}_L t_R \bar{t}_R t_L$), leading to the SM at the electroweak scale $v \approx 246$ GeV [143]. The scale $\Lambda = \mathcal{O}(\text{TeV})$ is estimated by using the top quark and Higgs boson masses and extrapolating the renormalization-group solution to the high-energy regime [144].

Composite bosons Π^f and fermions F^f spectra at the Λ scale offer a vast range of new searches and tests of the SM, as shown in [17]. In this article, we study the phenomenological analysis of composite boson states $\Phi \sim (\bar{\ell}_R q_L)$ with fractional electric charge, or LQ, as listed in Table I. Their SM gauge charges are the sum of the SM gauge charges of their fermionic constituents. The gauge-invariant kinetic Lagrangian is

$$(D_\mu \Phi)^\dagger (D_\mu \Phi) + M_\Pi^2 \Phi^\dagger \Phi, \quad (1)$$

with covariant derivative,

$$D_\mu = \partial_\mu + ig_1 Y B_\mu + \frac{1}{2} ig_2 \sigma_i W_\mu^i + ig_3 T^a G_\mu^a \quad (2)$$

where Y is the LQ hypercharge, σ_i are the standard Pauli matrices and T^a are the Gell-Mann matrices. Moreover, g_1 , g_2 , and g_3 are the SM gauge couplings for the respective group. In Eq. 1 $SU_c(3)$ triplet LQ bosons form $SU_L(2)$ doublets. Identification of doublets in terms of hypercharge

is given as $\Pi_{1/6}^a = \begin{pmatrix} \Pi_{u_a}^{2/3} \\ \Pi_a^{-1/3} \end{pmatrix}$ and $\Pi_{7/6}^a = \begin{pmatrix} \Pi_a^{5/3} \\ \Pi_{d_a}^{2/3} \end{pmatrix}$. The effective coupling between a LQ composite boson and its two constituents can be written as effective contact interactions,

$$\mathcal{L}_{CI} = g_{\Pi_{5/3}} (\bar{e}_R u_{La}) \Pi_a^{-5/3} + g_{\Pi_{1/3}} (\bar{\nu}_R^e d_{La}) \Pi_a^{1/3} + g_{\Pi_{-2/3}} (\bar{\nu}_R^e u_{La}) \Pi_{u_a}^{-2/3} + g_{\Pi_{-2/3}} (\bar{e}_R d_{La}) \Pi_{d_a}^{-2/3} + \text{h.c.} \quad (3)$$

where the LQ effective Yukawa coupling $g_{\Pi_i} = (F_{\Pi_i}/\Lambda)^2 \sim \mathcal{O}(1)$. The g_{Π_i} parameter defines the decay width (as calculated in [17] for composite bosons with integer charge) via the formula $\Gamma(q\ell) = (g_{\Pi_i}^2 m_{\Pi})/16\pi$ that coincides with the general formula used for scalar LQ (see [147]). For the sake of simplicity and to align to the notation commonly used in experiments (see e.g. [7, 74]) we will use λ to stand for g_{Π_i} in the sections below. The effective interacting Lagrangian (1-3) at the scale Λ is dimension-4 renormalizable, namely independent from the cutoff Λ_{cut} . We tabulate the four quark-lepton composite bosons $\Pi_a^{5/3}$, $\Pi_a^{-1/3}$, $\Pi_{u_a}^{2/3}$ and $\Pi_{d_a}^{2/3}$, identified by constituent fermions and SM gauge charges. Their conjugated fields are $(\Pi_a^{5/3})^\dagger = \Pi_a^{-5/3}$, $(\Pi_a^{-1/3})^\dagger = \Pi_a^{1/3}$ and $(\Pi_{u_a}^{2/3})^\dagger = \Pi_{d_a}^{-2/3}$, and $(\Pi_{d_a}^{2/3})^\dagger = \Pi_{u_a}^{-2/3}$. The renormalized LQ bosons $\Pi_a^Q = Z_{\Pi}^{-1/2} \bar{\ell}_R q_{La}$ with the form-factor $Z_{\Pi}^{-1/2} = (\sqrt{4\pi}/F_{\Pi})^2$ have the same dimension [*energy*] of elementary boson fields. Their masses $M_{\Pi} \propto \Lambda$ and decay constants $F_{\Pi} \propto \Lambda$, due to the composite dynamics at the scale Λ . These LQ states have baryon number $B = 1/3$ and lepton number $L = -1$, corresponding to R_2 and \tilde{R}_2 states in the LQ nomenclature [145, 146], which do not suffer interference with SM processes as pointed out in [83]. The spectra in Table (I), interactions (3), can be generalized by $\nu^e, e, u, d \rightarrow \nu^\mu, \mu, c, s$ for the second generation, and $\nu^e, e, u, d \rightarrow \nu^\tau, \tau, t, b$ for the third generation.

Although coupling G_{cut} and the composite scale Λ are unique, the coupling g_{Π_i} and mass M_{Π_i} have different values but are similar and related across generations. The main reason is that, in the four-fermion interactions, the fermion fields $\psi_{L,R}^f$ are SM gauge eigenstates. While in the ground state, they mix in different charged sectors and generations by unitary transformations $U_{L,R}^{\nu,\ell,u,d}$ [9]. Therefore, LQ states in different generations mix, provided they have the same SM charges of Table I. For example, $\Pi_a^{5/3} (\bar{e}_R u_{La})$ exhibits mixing amongst the LQ states $(\bar{\mu}_R c_{La})$ and $(\bar{\tau}_R t_{La})$. In addition to the Yukawa coupling (3), it can also couple to the lepton and quark in the second and third generations via flavor-mixed Yukawa couplings,

$$g_{\Pi_{5/3}} (U_R^\dagger U_L)_{1,2} (\bar{\mu}_R c_{La}) \Pi_a^{-5/3} + g_{\Pi_{5/3}} (U_R^\dagger U_L)_{1,3} (\bar{\tau}_R t_{La}) \Pi_a^{-5/3}, \quad (4)$$

where the flavor-suppressed factors $(U_R^\dagger U_L)_{1,3} < (U_R^\dagger U_L)_{1,2} < 1$ stand for the CKM-like mixing matrix elements between the first and other generations. The same discussions apply to other LQ states in Table I. Other flavor-mixed Yukawa couplings are possible, as long as they preserve

SM gauge symmetries. For these reasons, LQ boson masses and Yukawa couplings should be different in generations and related by an unknown mixing matrix $(U_{L,R}^{\nu,\ell,u,d})^\dagger U_{L,R}^{\nu,\ell,u,d}$, in analogy to the CKM matrix in the quark sector and PMNS matrix in the lepton sector. We treat different composite boson masses M_{Π_i} and Yukawa couplings g_{Π_i} as theoretical parameters. The constraint $g_{\Pi_i}^2 < 8\pi/\sqrt{3}$ is inferred by studying the unitarity problem [148].

These LQ bosons (Table I) and interactions (2-3) are the counterparts of color singlets $\Pi^{0,\pm}$ in Table V and interactions (26-28) of Ref. [17] by exchanging $e_{L,R} \leftrightarrow d_{L,R}^a$ and $\nu_{L,R}^e \leftrightarrow u_{L,R}^a$. The parameter spaces of Yukawa couplings g_{Π_i} and masses M_{Π_i} for investigating $\Pi^{0,\pm}$ are the same as those of LQ bosons up to the aforementioned mixing matrix elements of the order of unity. The differences are only the initial states' parton density functions (PDFs) used and the final states detected. For color singlets $\Pi^{0,\pm}$, there are decay (production) channels to (from) SM gauge bosons W, Z and γ , while color LQ states can be produced by gluon splitting or via a lepton-quark vertex. Analogously to the studies of composite fermions [17], we will discuss composite LQ fermions in a separate article, e.g. $F_R \sim \ell_R \Phi$ or $q_R \Phi$, interacting with SM gauge bosons and decaying to $\ell_R(q_R) + \Phi \rightarrow \ell_R(q_R) + \bar{\ell}_R + q_L$.

III. SIGNAL IMPLEMENTATION AND SAMPLES GENERATION

To generate signal and background events, we utilize MadGraph5 aMC@NLO[149], incorporating the gauge (Eq. 1) and the contact (Eq. 3) interaction terms described in the previous section via the Feynrules package [150] as a Universal FeynRules Output (UFO) module [151]. Subsequently, we generate Monte Carlo (MC) samples for both the signal and SM background processes via MadGraph5 aMC@NLO, then use Pythia 8.2 [152] for including initial and final parton showering and fragmentation. The Madgraph implementation includes the b quark in our proton definition, and the interactions have been implemented up to the 3rd fermion generation with the corresponding couplings.

In this article, we consider LQs with a charge of $5/3$ that couple to electron- u quark (λ_{eu}) and muon- c quark ($\lambda_{\mu c}$) pairs for the signal generation. The signal process is generated with two types of beam hypotheses: proton-proton (pp) and photon-proton (γp). For the pp LQ production, the NNPDF31-lo-as-0118 [153] PDF is used. For the γp collisions, we choose the MRST2004qed-proton PDF [154]. This decision is motivated by our aim to distinguish between the elastic and inelastic contributions of the photon. The NNPDF set previously mentioned incorporates both the elastic and inelastic contributions (as does the LUX PDF [155]), rendering it impractical to separate the

two components. The MRST2004qed PDF allows for the separation of the elastic and inelastic contributions with the configurations available in Madgraph. In our studies, we simulate the processes $pp \rightarrow \ell^+\ell^-$ plus 0, 1, 2, or at least 3 jets to incorporate the standard production modes in Fig. 1 (a - c) and the new production modes that are presented in the subsequent section. For the photon-induced processes, we consider $\gamma p \rightarrow \ell^+\ell^-$ plus 1 jet to focus our study on elastic versus inelastic contribution only.

The center-of-mass energy is set to 13 TeV. The values of λ vary in the range [0.5-2.5] in steps of 0.5. For the LQ masses, we consider values in the ranges (in TeV) [1.00-2.00] in steps of 0.25, [2.00, 10.00] in steps of 0.50, plus 20.00 and 30.00 TeV. Extra jets in the production of the LQ may originate from either gluons or quarks. The former corresponds to initial or final state radiation emitted in one of the well-searched tree-level diagrams, while the latter may give rise to novel mechanisms to generate LQs. We note that both scenarios can contribute to the overall signal, necessitating the avoidance of double counting of events among different processes. To achieve this, in the production of the signal samples, we employ the matrix element-parton shower matching technique known as MLM matching [156]. We set a matching scale at 30 GeV and ensure appropriate overlap removal in the differential jet rates of our samples. We have verified that the cross-sections obtained using our implemented model are consistent within 1% with those yielded by the models LQ-UFO [157], commonly used in analyses at LHC [7], using the same generator configurations and relying on the resonant pair production mode (Fig. 1 (c)) that does depend on α_s only.

IV. EXCLUSIVE LQ PRODUCTION

In this section, we explain LQ production in detail, emphasizing the mechanisms where LQs appear with additional jets compared to the well-established modes depicted in Fig. 1. We refer to this as “exclusive” LQ production, drawing an analogy to the nomenclature utilized in the study of inelastic scattering, where every reaction product is interested. Our examination of the numerous Feynman diagrams reveals three distinct cases of interest: (1) the splitting of a gluon into two quarks, one of which participates in the LQ generation, the other appearing as an additional jet; (2) the emission of a gluon from a parton that contributes to the LQ formation through separation into two quarks, with the original radiating parton and one of the gluon’s quarks ending as additional jets; (3) the exchange of a lepton that may lead to up to two additional jets. We remark that, although we are highlighting these possibilities in the context of the LQ particle, they

apply to any SM and BSM particle that permits the relevant couplings to quarks and leptons. It is also possible to have the emission of a gluon, arising from initial or final state radiation, that subsequently manifests as an additional jet (or two jets if it divides into quarks) and does not couple to the LQ. Although this latter occurrence also augments the jet multiplicity compared to the reference modes at the Born level, this scenario does not introduce new production processes, as it is anticipated within the hadronic environment of the LHC for any mechanism. The third instance above has been previously discussed in relation to pair production [78, 79] only, although it may occur also in t-channel and single production, and it introduces two additional new physics vertices that enhance the cross-section rapidly with respect to λ . The generation of a LQ initiated via a lepton is a unique production mode, and we treat it in the next sub-section.

The t-channel process studied in literature refers to the diagram in Fig. 1 (a) where the LQ interacts with two valence quarks in the initial state. However, such a production mode may be induced from the initial-state gluon splitting in either one or both incoming protons, as indicated in Fig. 2 (a, b). Another possibility is that a gluon or a lepton is exchanged, as illustrated in Fig. 2 (c, d), or a combination of the previous two cases, see Fig. 2 (e, f). Single LQ production is displayed on the diagrams in Fig. 1 (b) where the LQ creation starts from a gluon and a quark. Cases of both initial gluon splitting or gluon emission from a parton are possible, as illustrated in Fig. 2 (g-m). Figure 2 (n, o) instead shows the case where a lepton is exchanged in the process. The quantum chromodynamic LQ pair production happens via a gluon that separates into two LQs, and the primary mode is shown in Fig. 1 (c). Extra jets in final states coming from two LQ decays can originate from processes like those shown in Fig. 2 (p, q), while an example with a lepton exchange is displayed in Fig. 2 (r).

The examples discussed above describe some of the possible modes to produce LQs with additional jets, and one can expect different variants allowed by cross-symmetry of the particles involved in the interaction vertices. We note that combining the instances (1), (2), (3), as in diagram Fig 2 (e,f), further increases the number of jets and such diagrams are indeed produced by MadGraph, although their production cross-section decreases as the number of jets increases.

In this study, we aim to understand the impact of these processes in addition to those usually considered in the LHC searches. To accomplish this, we compare the cross-sections for t-channel, single, and pair production in Fig. 1 (a - c) to those obtained in the exclusive LQ production, which is shown in Fig. 3 for λ_{eu} (left) and $\lambda_{\mu c}$ (right) for a coupling value of 1.0. We observe a behavior that is consistent with the PDFs of the proton. At lower LQ masses, where the gluons in the proton dominate, the processes described above significantly contribute. For λ_{eu} there is

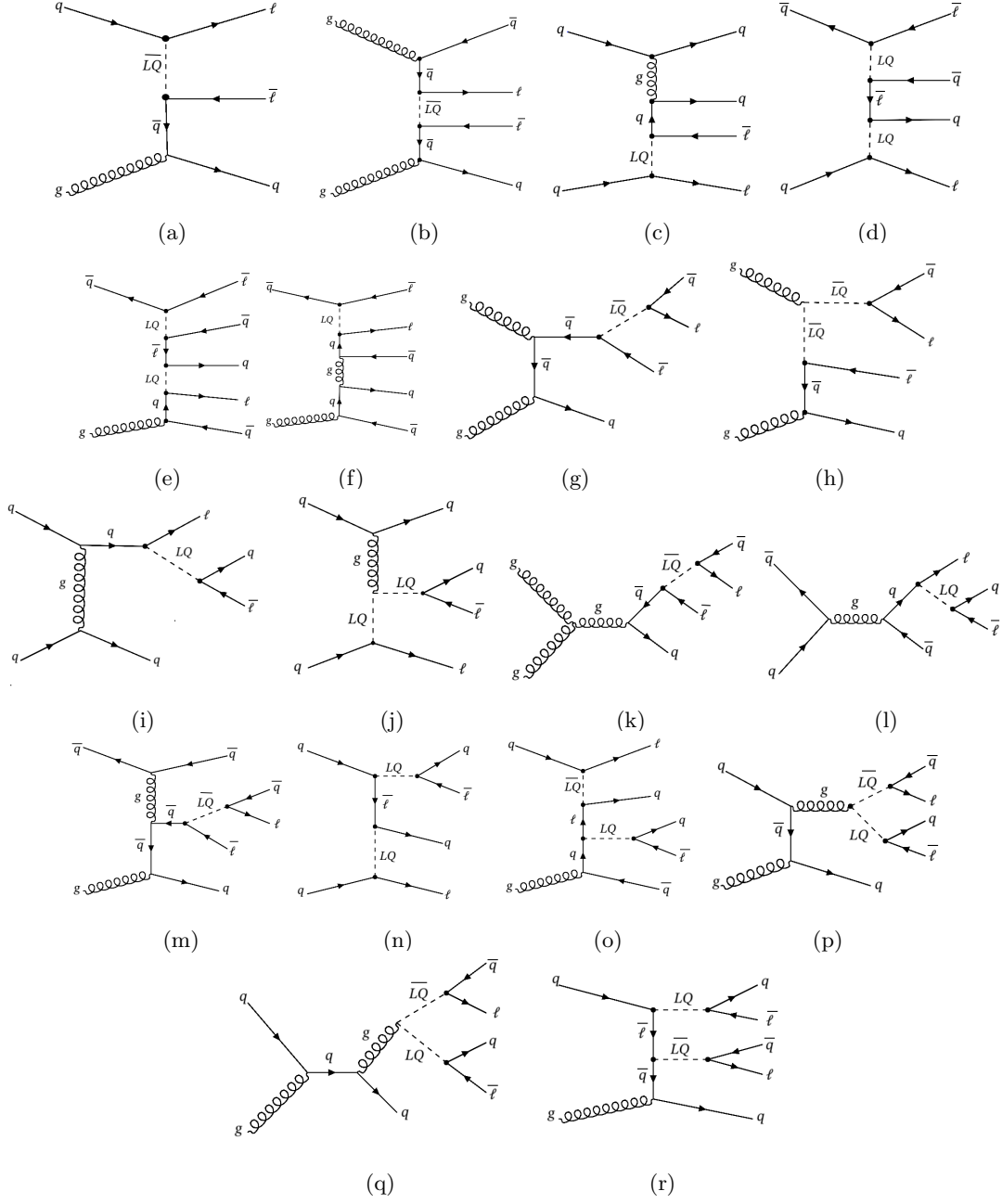


FIG. 2: Examples of Feynman diagrams for leptoquarks originating via one of the three mechanisms highlighted in exclusive production: (i) the splitting of a gluon into two quarks, (ii) the emission of a gluon from a parton, and (iii) the exchange of a lepton. They are illustrated for t-channel (a-f), single (g-o), and pair (p-r) production of leptoquarks.

an enhancement of the exclusive cross-section compared to the sum of the cross-sections from the processes in Fig. 1 (a - c) of about 40% for a LQ masses of 1 TeV and a coupling value of 1. For $\lambda_{\mu c}$ it is enhanced by a factor of 13 for the same mass and coupling. This is because for λ_{eu} the

LQ is coupled to a u quark, while for $\lambda_{\mu c}$ to a c quark. We anticipate that the higher the quark generation the greater this contribution, which is thus particularly relevant for LQs coupling to a lepton and s , c , b , t quarks. Because of this, below we focus only on the study of the sensitivity for the case where the LQ couples to a muon - c quark pair. This ratio tends to converge to 1 at higher LQ masses for two reasons: the presence of gluons taper off and valence quarks dominate; there is a kinematic limit due to LHC center-of-mass energy for the production of resonant single and pair LQs, while such a constraint is less stringent in the t-channel case. These two points imply that at higher and higher masses and λ , the dominant contribution will come from the t-channel process, as we observe here.

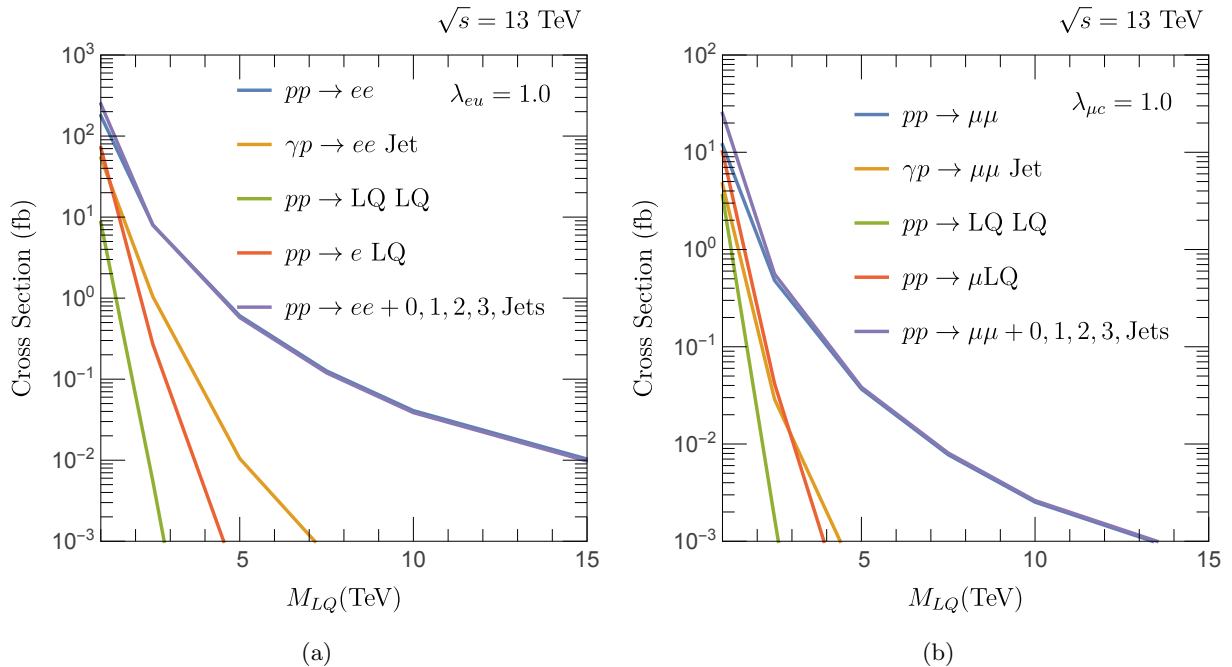


FIG. 3: Cross-sections for different leptoquark production modes, for a coupling of the electron to the u quark $\lambda_{eu} = 1$, (a) and for a coupling of the muon to the c quark $\lambda_{\mu c} = 1$, (b).

A. Lepton initiated LQ production

The idea that LQs may be produced from a lepton that stems via vacuum fluctuations in the proton was proposed a long time ago in literature [80]. It has become recently feasible due to an improved estimate of the lepton density functions (LDFs) [86] and it has been used at CMS [127]. Here, we discuss how such a process enters our view to proceed to a global search for LQs.

The first point to remark on is that the works [86, 127] study s-channel LQ production only. However, t-channel LQ exchange is possible and should be considered. The second aspect to note is that one can consider lepton-induced processes using the exclusive production approach introduced here by noting that all the processes illustrated in Fig. 2 and discussed above are equally possible by simply substituting a gluon that splits into two quarks with a photon that splits into two leptons.

There is another more general consideration to mention in relation to the lepton that produces the LQ, and it concerns whether its mother particle, the photon, for example, stems from elastic (the proton remains intact, Fig. 4 (a)) or inelastic (the proton does not remain intact, Fig. 4 (b)). For the elastic case, we define one of the protons to be a photon, while for the inelastic case, we include the photon in the proton without changing the default type. For $\lambda_{\mu c} = 1$, we see that the ratio of the contribution to the cross-section from the elastic to the inelastic case is about 27%. Despite the lower ratio for the elastic case, we point out that a dedicated search relying on the elastic case would have an enormous advantage in mitigating the SM background, as pointed out in several investigations [158].

By comparing the total cross-section obtained summing up both elastic and inelastic cases with that using the LDFs as in Fig.1 (d), we see that the two are consistent within 20%.

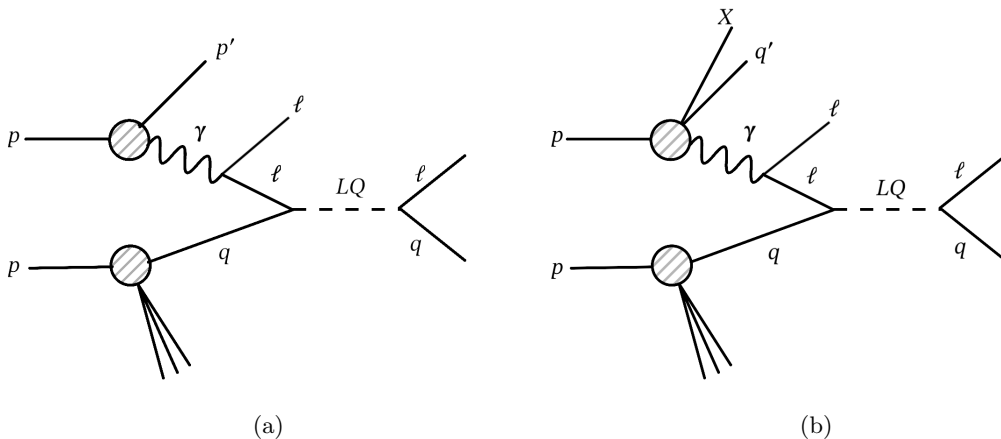


FIG. 4: Feynman diagrams for the single leptoquark production for the cases where a photon that splits into two leptons is radiated by the proton elastically (a) or inelastically (b).

V. SEARCH STRATEGY

The signal we look for produces a signature with two leptons in the final state plus a given number of jets (0, 1, 2, or at least 3). The samples described in Section III for the $\lambda_{\mu c}$ coupling, as

discussed in Section IV, are used in the event selection. The events pass the signal selection if they satisfy the following baseline requirements: exactly two muons with transverse momentum $p_T > 20$ GeV, pseudorapidity $|\eta| < 2.5$, and invariant mass greater than 120 GeV; missing transverse energy lower than 50 GeV; and no jets originating from b quarks. We find that the selection efficiency is about 30% or higher from masses of 1 TeV and all coupling values.

Jets are chosen to have $p_T > 20$ GeV and $|\eta| < 5$, and to be spatially separated from the selected muons by $\Delta R > 0.4$, where $\Delta R = \sqrt{(\Delta\eta)^2 + (\Delta\phi)^2}$ and ϕ is the azimuthal angle. We do not set any condition on a minimal number of jets, as we separate the signal region events into categories with 0, 1, 2, or at least 3 jets.

In Fig. 5 we show the distribution from pp events from processes including two jets in the two-dimensional plane of χ and S_T , where $\chi = e^{|\eta_1 - \eta_2|}$ and η_1, η_2 are the pseudorapidities of the two muons, while S_T is defined as the sum of the scalar p_T of the leptons and selected jets. The plots are shown for two signals hypotheses, with LQ mass equal to 2 (4) TeV and $\lambda_{\mu c}$ coupling of 1.0 (2.5) on the left (center) and the SM background on the right.

Background events are generated at leading order (LO) with PDF NNPDF31-lo-as-0118 [153], and scaled using next-to-leading-order (NLO) cross-sections where appropriate. The processes we consider are $W + \text{jets}$ ($W \rightarrow l + \nu$), Drell-Yan (charged lepton decays) + jets, single top, $t\bar{t}$, and diboson (WW, WZ, and ZZ). Background processes are generated with sufficiently high jet multiplicities to yield an accurate comparison against our targeted signal. Generator-level production is then interfaced with Pythia 8.2 [152] for parton showering and hadronization using the Monash 2013 tune [159]. Detector response simulation is obtained via the Delphes framework [160]. As in our signal events, jet matching is implemented using the MLM algorithm to avoid double counting of events after showering and hadronization.

VI. EXPECTED SENSITIVITY AT LHC AND HL-LHC

The distributions of the χ and S_T variable per jet multiplicity for the events of the signal regions are used as the final discriminant between the LQ signal and the background. We sum up signal events from both the pp and γp collisions, accounting for production cross-section, efficiency, and luminosity, and use a profile-binned likelihood statistical test [161] for assessing the expected signal significance. Nuisance parameters encompassing systematic uncertainties are introduced for the signal (background), incorporating log-normal priors. We follow the same prescriptions used in the published LQ searches [104, 106] and we briefly summarize them below. The uncertainties arising

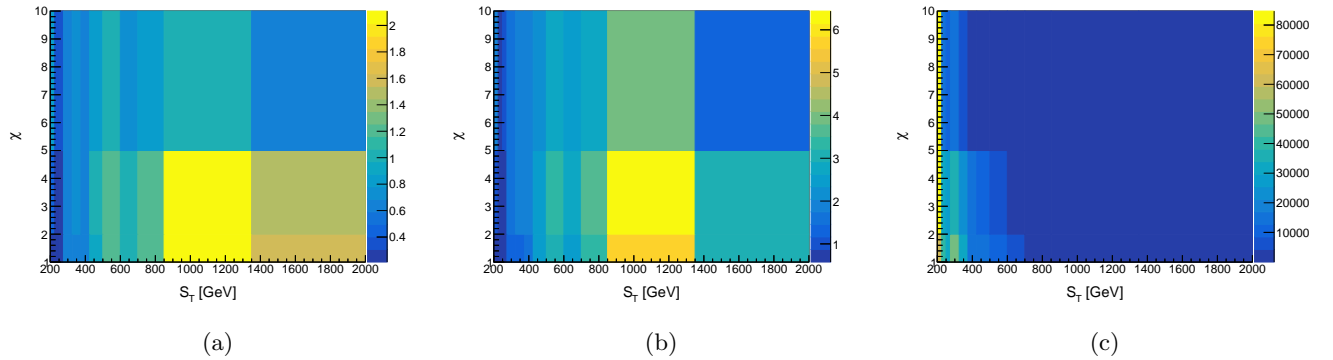


FIG. 5: Distributions of the pp events passing the baseline selection specified in the text and requiring two jets in the two-dimensional plane of angular χ and energy S_T observables defined in the paper. The plots are shown for two signals hypotheses with leptoquark mass equal to 2 (4) TeV and $\lambda_{\mu c}$ coupling of 1.0 (2.5) on the left (center) and the SM background on the right.

from the selection of the parton distribution function in the MC production is 2.8% (3.0%), while that related to additional interaction vertices in the event amount to 0.2% (1.0%). The uncertainties associated with jet and lepton energy resolution are 0.1% (1.7%) and 0.2% (5.3%), respectively. Additionally, jet and lepton energy scale uncertainties are included with values of 0.5% (0.9%) and 1.5% (2.5%). The uncertainties for leptonic reconstruction and identification efficiency stand at 3.0% and 1.3% (0.3%). For the calculation of expected significance the “Combine Tool” is used [162]. In Fig. 6, we present contour plots of the expected significance in the two-dimensional plane of the coupling λ and the mass of the LQ. These plots are obtained at the center-of-mass energy of 13 TeV and an integrated luminosity of 300 fb^{-1} (left), as a possible value of the luminosity expected by the end of the ongoing data-taking period at the LHC referred to as Run 3, and varying luminosity assumptions (right) at 140 (blue), 300 (red), 3000 (green) fb^{-1} , for the 5σ (plain line) and 2σ (dashed line) significance levels. The vertical lines show the most recent exclusion limits results at 95% confidence level from a search for LQs from ATLAS [94] (black dashed) and CMS [106] (violet plain) collaborations scaled for 300 (left) and 3000 (right) fb^{-1} . The results obtained with the exclusive LQ approach report a 5 (2) σ significance for LQ masses up to 2.0, 2.2, 2.5 (2.3, 2.4, 3.4) TeV, for $\lambda_{\mu c} = 0.5$, and 8.0, 9.7, 18.6 (14.9, 17.5, 27.3) TeV, for $\lambda_{\mu c} = 2.5$, at 140, 300, 3000 fb^{-1} . While ATLAS and CMS scaled results would exclude a LQ coupling to a muon - c quark pair up to masses of 1.7, 1.8, 2.2, and 1.8, 1.9, 2.3 TeV regardless of the coupling value and for the same luminosity scenarios. With the strategy developed in this article, we obtain that the 2σ significance with 140 fb^{-1} is comparable to the scaled upper limit

on the LQ mass expected by ATLAS and CMS with 3000 fb^{-1} , for the lowest coupling value that we consider.

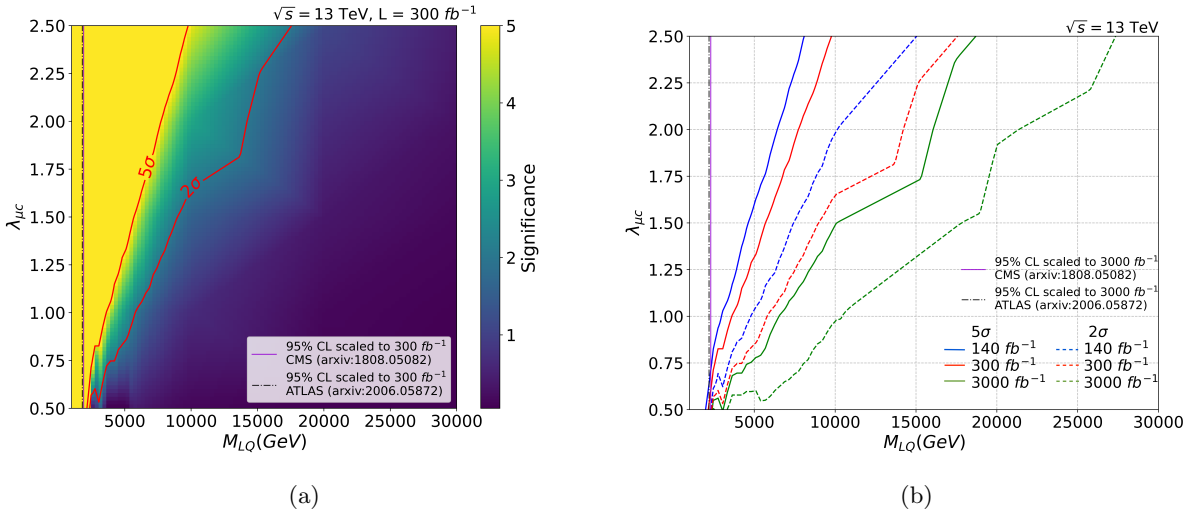


FIG. 6: Signal significance in the plane of the coupling $\lambda_{\mu c}$ and the mass of the LQ using pp and γp events at $\sqrt{s} = 13 \text{ TeV}$ expected for 300 fb^{-1} (left) and different luminosity scenarios (right).

The colored solid and dashed lines represent 5 and 2 σ levels for the analysis presented in this text, while the vertical lines show the most recent exclusion limits results at 95% confidence level from a search for LQs from ATLAS [94] (black dashed) and CMS [106] (violet plain) collaborations scaled for 300 (left) and 3000 (right) fb^{-1} .

VII. SUMMARY AND REMARKS

As the LHC proceeds in collecting more data at the utmost center-of-mass energy and with the slow relative increase in luminosity anticipated by the High-Luminosity initiative of the accelerator, the absence of compelling evidence for new physics prompts a critical consideration. It becomes increasingly important to assess whether existing searches have thoroughly investigated all conceivable paths or whether new approaches may still be formulated to enhance the discovery potential and to unlock access to a phase space that was not considered reachable before.

In this paper, we have tackled this question by conducting a comprehensive study of the well-motivated, known, and extensively researched LQ particle. Although we carry out a study that is valid for any model, we have relied on a novel scenario of LQ composite particles via the NJL model with effective strong four-fermion couplings [10, 142]. This model introduces a different

mechanism for compositeness than those considered at LHC [88, 163–169] and offers a broad variety of new composite particles: integer charge bosons $\Pi^f \sim (\bar{\psi}_R^f \psi_L^f)$ and fermions $F_R^f \sim \psi_R^f (\bar{\psi}_R^f \psi_L^f) \sim \psi_R^f \Pi^f$ [17], fractional charge bosons such as the LQ bosons studied here, composite LQ fermions, and composite Higgs to be studied in future works. These could manifest in signatures that have not yet been explored at the LHC.

Compared to existing investigations that rely on the primary LQ production modes in Fig. 1, for the first time, we have examined the impact on the sensitivity of the search for particles when they are produced in association with additional jets. We have found that several new mechanisms are possible besides the classical pair, single, and Drell-Yan non-resonant LQ generation, as discussed in Section IV and illustrated in Fig. 2. We refer to the ensemble of all allowed processes as “exclusive” LQ production, in analogy to the terminology adopted in inelastic scattering, where all reaction products are involved.

We have found that the exclusive cross-section surpasses that of the mechanisms in Fig. 1 by about a factor 13 for a LQ coupling to muon - c quark pair, and 40, for the coupling to electron - u quark pair at a mass of 1 TeV and a coupling value of 1, as shown in Fig. 3. The enhancement turns out to be greater for LQ coupling to higher quark generation, rendering the exclusive production particularly interesting for a LQ decaying to a lepton and a s , c , b , t quarks. Moreover, we have expanded this approach referring to LDFs and we also pursue an unprecedented distinction between inelastic and elastic modes, the former resulting in about 80% of the total although the latter would benefit from a reduced background contamination [158].

Based on the view of exclusive LQ production, we have designed a new global strategy to intercept t-channel, single, and pair signal generation at different jet multiplicities and using simultaneous observables that exploit the expected event energy (S_T) and angular (χ) distributions. We anticipate that an optimal combination of the energetic and angular variables would be exploited by relying on machine learning techniques. As shown in Fig. 6, we achieve a significance of 5 (2) σ for LQ masses up to 2.0, 2.2, 2.5 (2.3, 2.4, 3.4) TeV, for $\lambda_{\mu c} = 0.5$, and 8.0, 9.7, 18.6 (14.9, 17.5, 27.3) TeV, for $\lambda_{\mu c} = 2.5$, at 140, 300, 3000 fb^{-1} . The significance of 2 σ with 140 fb^{-1} is comparable to the scaled upper limit on the LQ mass expected by ATLAS [94] and CMS [106] with 3000 fb^{-1} for the lowest coupling value that we consider.

These results are notably relevant for BSM scenarios with preferential couplings to higher fermion generations, including models that have the potential to explain some of the persistent, yet to be confirmed, anomalies in high energy physics (such as the aforementioned $B \rightarrow D^*$ and $(g-2)_\mu$ precision measurements), as they allow to probe a much wider region of the LQ coupling-mass plane

compared to traditional searches and especially for couplings to higher generation fermions.

In light of these results and the discovery reach, we deem that the exclusive LQ search should be considered in future investigations at the LHC. We further point out that the three instances that open up new production mechanisms and the elastic/inelastic processes described in Section IV apply to any SM and BSM (e.g. heavy neutrinos, Z' -like, W' -like, and so on) particle that permits the relevant couplings to quarks and leptons.

ACKNOWLEDGMENTS

This work has received funding from the INFN project ENP (Exploring New Physics). J. Gaglione, A. Gurrola, and F. Romeo acknowledge the funding received from the Physics and Astronomy department at Vanderbilt University and the US National Science Foundation. This work is supported in part by NSF Award PHY-1945366 and a Vanderbilt Seeding Success Grant. The work of M. Presilla is supported by the Alexander von Humboldt-Stiftung. H. Sun is supported by the National Natural Science Foundation of China (Grant No.12075043).

-
- [1] ATLAS Collaboration (ATLAS), *JHEP* **03**, 145 (2020), [arXiv:1910.08447 \[hep-ex\]](#).
 - [2] ATLAS Collaboration (ATLAS), *Phys. Rev. D* **104**, 112005 (2021), [arXiv:2108.07665 \[hep-ex\]](#).
 - [3] ATLAS Collaboration (ATLAS), *Phys. Lett. B* **798**, 134942 (2019), [arXiv:1904.12679 \[hep-ex\]](#).
 - [4] CMS Collaboration (CMS), Preprint CERN-EP-2022-037 (2022) submitted to Physical Review D. All figures and tables can be found at <http://cms-results.web.cern.ch/cms-results/public-results/publications/EXO-20-008> (CMS Public Pages), [arXiv:2205.01835 \[hep-ex\]](#).
 - [5] CMS Collaboration (CMS), *JHEP* **07**, 208 (2021), [arXiv:2103.02708 \[hep-ex\]](#).
 - [6] CMS Collaboration (CMS), *JHEP* **05**, 033 (2020), [arXiv:1911.03947 \[hep-ex\]](#).
 - [7] CMS Collaboration (CMS), *Phys. Lett. B* **819**, 136446 (2021), [arXiv:2012.04178 \[hep-ex\]](#).
 - [8] CMS Collaboration (CMS), Preprint CERN-EP-2022-105 (2022) submitted to Physical Review Letters. All figures and tables can be found at <http://cms-results.web.cern.ch/cms-results/public-results/publications/EXO-21-003> (CMS Public Pages), [arXiv:2206.08956 \[hep-ex\]](#).
 - [9] S.-S. Xue, *JHEP* **11**, 072 (2016), [arXiv:1605.01266 \[hep-ph\]](#).
 - [10] S.-S. Xue, *JHEP* **05**, 146 (2017), [arXiv:1601.06845 \[hep-ph\]](#).
 - [11] H. B. Nielsen and M. Ninomiya, *Nucl. Phys. B* **185**, 20 (1981), [Erratum: *Nucl.Phys.B* 195, 541 (1982)].
 - [12] H. B. Nielsen and M. Ninomiya, *Phys. Lett. B* **105**, 219 (1981).
 - [13] H. B. Nielsen and M. Ninomiya, *Int. J. Mod. Phys. A* **6**, 2913 (1991).

- [14] S.-S. Xue, *Phys. Lett. B* **665**, 54 (2008), [arXiv:0804.4619 \[hep-th\]](#).
- [15] S.-S. Xue, *Phys. Lett. B* **682**, 300 (2009), [arXiv:0902.3407 \[hep-th\]](#).
- [16] S.-S. Xue, *Phys. Rev. D* **82**, 064039 (2010), [arXiv:0912.2435 \[hep-th\]](#).
- [17] R. Leonardi, O. Panella, F. Romeo, A. Gurrola, H. Sun, and S.-S. Xue, *Eur. Phys. J. C* **80**, 309 (2020), [arXiv:1810.11420 \[hep-ph\]](#).
- [18] A. M. Sirunyan *et al.* (CMS), *Phys. Lett. B* **775**, 315 (2017), [arXiv:1706.08578 \[hep-ex\]](#).
- [19] L. Pacioselli, O. Panella, M. Presilla, and S. S. Xue, *Journal of High Energy Physics* **2023**, 54 (2023).
- [20] J. C. Pati and A. Salam, *Phys. Rev. D* **8**, 1240 (1973).
- [21] J. C. Pati and A. Salam, *Phys. Rev. D* **10**, 275 (1974).
- [22] H. Georgi and S. L. Glashow, *Phys. Rev. Lett.* **32**, 438 (1974).
- [23] H. Fritzsch and P. Minkowski, *Ann. Phys.* **93**, 193 (1975).
- [24] S. Gershtein, A. Likhoded, and A. Onishchenko, *Physics Reports* **320**, 159 (1999).
- [25] I. Dorsner and P. Fileviez Perez, *Nucl. Phys. B* **723**, 53 (2005), [arXiv:hep-ph/0504276](#).
- [26] S. Dimopoulos and L. Susskind, *Nucl. Phys. B* **155**, 237 (1979).
- [27] S. Dimopoulos, *Nucl. Phys. B* **168**, 69 (1980).
- [28] E. Farhi and L. Susskind, *Phys. Rept.* **74**, 277 (1981).
- [29] K. D. Lane and M. V. Ramana, *Phys. Rev. D* **44**, 2678 (1991).
- [30] B. Schrempp and F. Schrempp, *Phys. Lett. B* **153**, 101 (1985).
- [31] B. Gripaios, *JHEP* **02**, 045 (2010), [arXiv:0910.1789 \[hep-ph\]](#).
- [32] G. R. Farrar and P. Fayet, *Phys. Lett. B* **76**, 575 (1978).
- [33] P. Ramond, *Phys. Rev. D* **3**, 2415 (1971).
- [34] Y. A. Golfand and E. P. Likhtman, *JETP Lett.* **13**, 323 (1971).
- [35] A. Neveu and J. H. Schwarz, *Nucl. Phys. B* **31**, 86 (1971).
- [36] D. V. Volkov and V. P. Akulov, *JETP Lett.* **16**, 438 (1972).
- [37] J. Wess and B. Zumino, *Phys. Lett. B* **49**, 52 (1974).
- [38] J. Wess and B. Zumino, *Nucl. Phys. B* **70**, 39 (1974).
- [39] P. Fayet, *Nucl. Phys. B* **90**, 104 (1975).
- [40] H. P. Nilles, *Phys. Rept.* **110**, 1 (1984).
- [41] R. Barbier, C. Bérat, M. Besançon, M. Chemtob, A. Deandrea, E. Dudas, P. Fayet, S. Lavignac, G. Moreau, E. Perez, and Y. Sirois, *Phys. Rept.* **420**, 1 (2005), [arXiv:hep-ph/0406039 \[hep-ph\]](#).
- [42] M. J. Baker *et al.*, *JHEP* **12**, 120 (2015), [arXiv:1510.03434 \[hep-ph\]](#).
- [43] J. P. Lees *et al.* (BaBar), *Phys. Rev. Lett.* **109**, 101802 (2012), [arXiv:1205.5442 \[hep-ex\]](#).
- [44] J. P. Lees *et al.* (BaBar), *Phys. Rev. D* **88**, 072012 (2013), [arXiv:1303.0571 \[hep-ex\]](#).
- [45] M. Huschle *et al.* (Belle), *Phys. Rev. D* **92**, 072014 (2015), [arXiv:1507.03233 \[hep-ex\]](#).
- [46] R. Aaij *et al.* (LHCb), *Phys. Rev. Lett.* **115**, 111803 (2015), [Erratum: *Phys.Rev.Lett.* 115, 159901 (2015)], [arXiv:1506.08614 \[hep-ex\]](#).
- [47] T. Mandal, S. Mitra, and S. Raz, *Phys. Rev. D* **99**, 055028 (2019), [arXiv:1811.03561 \[hep-ph\]](#).

- [48] B. Dumont, K. Nishiwaki, and R. Watanabe, *Phys. Rev. D* **94**, 034001 (2016), [arXiv:1603.05248 \[hep-ph\]](#).
- [49] C.-H. Chen, T. Nomura, and H. Okada, *Phys. Lett. B* **774**, 456 (2017), [arXiv:1703.03251 \[hep-ph\]](#).
- [50] R. Barbieri, C. W. Murphy, and F. Senia, *Eur. Phys. J. C* **77**, 8 (2017), [arXiv:1611.04930 \[hep-ph\]](#).
- [51] M. Tanaka and R. Watanabe, *Phys. Rev. D* **87**, 034028 (2013), [arXiv:1212.1878 \[hep-ph\]](#).
- [52] S. Iguro and Y. Omura, (2023), [arXiv:2306.00052 \[hep-ph\]](#).
- [53] A. Flórez, J. Jones-Pérez, A. Gurrola, C. Rodriguez, and J. Peñuela Parra, (2023), [arXiv:2307.11070 \[hep-ph\]](#).
- [54] B. Abi *et al.* (Muon g-2), *Phys. Rev. Lett.* **126**, 141801 (2021), [arXiv:2104.03281 \[hep-ex\]](#).
- [55] G. W. Bennett *et al.* (Muon g-2), *Phys. Rev. D* **73**, 072003 (2006), [arXiv:hep-ex/0602035](#).
- [56] G. W. Bennett *et al.* (Muon g-2), *Phys. Rev. D* **73**, 072003 (2006), [arXiv:hep-ex/0602035](#).
- [57] M. Bauer and M. Neubert, *Phys. Rev. Lett.* **116**, 141802 (2016), [arXiv:1511.01900 \[hep-ph\]](#).
- [58] A. Greljo, P. Stangl, and A. E. Thomsen, *Phys. Lett. B* **820**, 136554 (2021), [arXiv:2103.13991 \[hep-ph\]](#).
- [59] M. Du, J. Liang, Z. Liu, and V. Q. Tran, (2021), [arXiv:2104.05685 \[hep-ph\]](#).
- [60] S. Parashar, A. Karan, Avnish, P. Bandyopadhyay, and K. Ghosh, *Phys. Rev. D* **106**, 095040 (2022), [arXiv:2209.05890 \[hep-ph\]](#).
- [61] S.-L. Chen, W.-w. Jiang, and Z.-K. Liu, *Eur. Phys. J. C* **82**, 959 (2022), [arXiv:2205.15794 \[hep-ph\]](#).
- [62] T. A. Chowdhury and S. Saad, *Phys. Rev. D* **106**, 055017 (2022), [arXiv:2205.03917 \[hep-ph\]](#).
- [63] S.-P. He, *Chin. Phys. C* **47**, 043102 (2023), [arXiv:2205.02088 \[hep-ph\]](#).
- [64] K. Cheung, W.-Y. Keung, and P.-Y. Tseng, *Phys. Rev. D* **106**, 015029 (2022), [arXiv:2204.05942 \[hep-ph\]](#).
- [65] S.-P. He, *Phys. Rev. D* **105**, 035017 (2022), [Erratum: *Phys.Rev.D* 106, 039901 (2022)], [arXiv:2112.13490 \[hep-ph\]](#).
- [66] I. Bigaran and R. R. Volkas, *Phys. Rev. D* **105**, 015002 (2022), [arXiv:2110.03707 \[hep-ph\]](#).
- [67] X. Wang, *JHEP* **08**, 243 (2022), [arXiv:2108.01279 \[hep-ph\]](#).
- [68] D. Zhang, *JHEP* **07**, 069 (2021), [arXiv:2105.08670 \[hep-ph\]](#).
- [69] P. Fileviez Perez, C. Murgui, and A. D. Plascencia, *Phys. Rev. D* **104**, 035041 (2021), [arXiv:2104.11229 \[hep-ph\]](#).
- [70] K. Ban, Y. Jho, Y. Kwon, S. C. Park, S. Park, and P.-Y. Tseng, *PTEP* **2023**, 013B01 (2023), [arXiv:2104.06656 \[hep-ph\]](#).
- [71] R. Pohl *et al.*, *Nature* **466**, 213 (2010).
- [72] C. S. Wood, S. C. Bennett, D. Cho, B. P. Masterson, J. L. Roberts, C. E. Tanner, and C. E. Wieman, *Science* **275**, 1759 (1997).
- [73] I. Dorsner, S. Fajfer, and A. Greljo, *JHEP* **10**, 154 (2014), [arXiv:1406.4831 \[hep-ph\]](#).
- [74] A. Hayrapetyan *et al.* (CMS), (2023), [arXiv:2308.07826 \[hep-ex\]](#).
- [75] A. Collaboration (ATLAS), (2023), [arXiv:2305.15962 \[hep-ex\]](#).

- [76] B. Diaz, M. Schmaltz, and Y.-M. Zhong, *JHEP* **10**, 097 (2017), [arXiv:1706.05033 \[hep-ph\]](#).
- [77] J. Blumlein, E. Boos, and A. Kryukov, *Z. Phys. C* **76**, 137 (1997), [arXiv:hep-ph/9610408](#).
- [78] I. Doršner, A. Lejlić, and S. Saad, *JHEP* **03**, 025 (2023), [arXiv:2210.11004 \[hep-ph\]](#).
- [79] I. Doršner, S. Fajfer, and A. Lejlić, *JHEP* **05**, 167 (2021), [arXiv:2103.11702 \[hep-ph\]](#).
- [80] J. Ohnemus, S. Rudaz, T. F. Walsh, and P. M. Zerwas, *Phys. Lett. B* **334**, 203 (1994), [arXiv:hep-ph/9406235](#).
- [81] T. Mandal, S. Mitra, and S. Seth, *JHEP* **07**, 028 (2015), [arXiv:1503.04689 \[hep-ph\]](#).
- [82] N. Raj, *Phys. Rev. D* **95**, 015011 (2017), [arXiv:1610.03795 \[hep-ph\]](#).
- [83] S. Bansal, R. M. Capdevilla, A. Delgado, C. Kolda, A. Martin, and N. Raj, *Phys. Rev. D* **98**, 015037 (2018), [arXiv:1806.02370 \[hep-ph\]](#).
- [84] M. Schmaltz and Y.-M. Zhong, *JHEP* **01**, 132 (2019), [arXiv:1810.10017 \[hep-ph\]](#).
- [85] A. Greljo and N. Selimovic, *JHEP* **03**, 279 (2021), [arXiv:2012.02092 \[hep-ph\]](#).
- [86] L. Buonocore, U. Haisch, P. Nason, F. Tramontano, and G. Zanderighi, *Phys. Rev. Lett.* **125**, 231804 (2020), [arXiv:2005.06475 \[hep-ph\]](#).
- [87] G. Aad *et al.* (ATLAS), (2023), [arXiv:2306.17642 \[hep-ex\]](#).
- [88] G. Aad *et al.* (ATLAS), *JHEP* **06**, 199 (2023), [arXiv:2303.09444 \[hep-ex\]](#).
- [89] (2023), [arXiv:2303.01294 \[hep-ex\]](#).
- [90] G. Aad *et al.* (ATLAS), *JHEP* **2306**, 188 (2023), [arXiv:2210.04517 \[hep-ex\]](#).
- [91] G. Aad *et al.* (ATLAS), *JHEP* **05**, 093 (2021), [arXiv:2101.12527 \[hep-ex\]](#).
- [92] G. Aad *et al.* (ATLAS), *JHEP* **06**, 179 (2021), [arXiv:2101.11582 \[hep-ex\]](#).
- [93] G. Aad *et al.* (ATLAS), *Eur. Phys. J. C* **81**, 313 (2021), [arXiv:2010.02098 \[hep-ex\]](#).
- [94] G. Aad *et al.* (ATLAS), *JHEP* **10**, 112 (2020), [arXiv:2006.05872 \[hep-ex\]](#).
- [95] G. Aad *et al.* (ATLAS), *Eur. Phys. J. C* **80**, 737 (2020), [arXiv:2004.14060 \[hep-ex\]](#).
- [96] M. Aaboud *et al.* (ATLAS), *JHEP* **06**, 144 (2019), [arXiv:1902.08103 \[hep-ex\]](#).
- [97] M. Aaboud *et al.* (ATLAS), *Eur. Phys. J. C* **79**, 733 (2019), [arXiv:1902.00377 \[hep-ex\]](#).
- [98] M. Aaboud *et al.* (ATLAS), *New J. Phys.* **18**, 093016 (2016), [arXiv:1605.06035 \[hep-ex\]](#).
- [99] G. Aad *et al.* (ATLAS), *Eur. Phys. J. C* **76**, 5 (2016), [arXiv:1508.04735 \[hep-ex\]](#).
- [100] G. Aad *et al.* (ATLAS), *JHEP* **06**, 033 (2013), [arXiv:1303.0526 \[hep-ex\]](#).
- [101] G. Aad *et al.* (ATLAS), *Eur. Phys. J. C* **72**, 2151 (2012), [arXiv:1203.3172 \[hep-ex\]](#).
- [102] G. Aad *et al.* (ATLAS), *Phys. Lett. B* **709**, 158 (2012), [Erratum: *Phys.Lett.B* 711, 442–455 (2012)], [arXiv:1112.4828 \[hep-ex\]](#).
- [103] G. Aad *et al.* (ATLAS), *Phys. Rev. D* **83**, 112006 (2011), [arXiv:1104.4481 \[hep-ex\]](#).
- [104] A. M. Sirunyan *et al.* (CMS), *Phys. Rev. D* **99**, 052002 (2019), [arXiv:1811.01197 \[hep-ex\]](#).
- [105] A. Tumasyan *et al.* (CMS), *Phys. Rev. D* **105**, 112007 (2022), [arXiv:2202.08676 \[hep-ex\]](#).
- [106] A. M. Sirunyan *et al.* (CMS), *Phys. Rev. D* **99**, 032014 (2019), [arXiv:1808.05082 \[hep-ex\]](#).
- [107] A. M. Sirunyan *et al.* (CMS), *Phys. Rev. Lett.* **121**, 241802 (2018), [arXiv:1809.05558 \[hep-ex\]](#).
- [108] A. M. Sirunyan *et al.* (CMS), *JHEP* **03**, 170 (2019), [arXiv:1811.00806 \[hep-ex\]](#).

- [109] A. M. Sirunyan *et al.* (CMS), *Eur. Phys. J. C* **80**, 3 (2020), [arXiv:1909.03460 \[hep-ex\]](#).
- [110] A. M. Sirunyan *et al.* (CMS), *Phys. Lett. B* **795**, 76 (2019), [arXiv:1811.10151 \[hep-ex\]](#).
- [111] A. M. Sirunyan *et al.* (CMS), *JHEP* **07**, 121 (2017), [arXiv:1703.03995 \[hep-ex\]](#).
- [112] V. Khachatryan *et al.* (CMS), *JHEP* **03**, 077 (2017), [arXiv:1612.01190 \[hep-ex\]](#).
- [113] V. Khachatryan *et al.* (CMS), *Phys. Rev. D* **93**, 032004 (2016), [arXiv:1509.03744 \[hep-ex\]](#).
- [114] V. Khachatryan *et al.* (CMS), *JHEP* **07**, 042 (2015), [Erratum: *JHEP* **11**, 056 (2016)], [arXiv:1503.09049 \[hep-ex\]](#).
- [115] V. Khachatryan *et al.* (CMS), *Phys. Lett. B* **739**, 229 (2014), [arXiv:1408.0806 \[hep-ex\]](#).
- [116] S. Chatrchyan *et al.* (CMS), *JHEP* **12**, 055 (2012), [arXiv:1210.5627 \[hep-ex\]](#).
- [117] S. Chatrchyan *et al.* (CMS), *Phys. Rev. D* **86**, 052013 (2012), [arXiv:1207.5406 \[hep-ex\]](#).
- [118] S. Chatrchyan *et al.* (CMS), *Phys. Lett. B* **703**, 246 (2011), [arXiv:1105.5237 \[hep-ex\]](#).
- [119] V. Khachatryan *et al.* (CMS), *Phys. Rev. Lett.* **106**, 201803 (2011), [arXiv:1012.4033 \[hep-ex\]](#).
- [120] V. Khachatryan *et al.* (CMS), *Phys. Rev. Lett.* **106**, 201802 (2011), [arXiv:1012.4031 \[hep-ex\]](#).
- [121] G. Aad *et al.* (ATLAS), *Phys. Lett. B* **830**, 137106 (2022), [arXiv:2112.08090 \[hep-ex\]](#).
- [122] V. Khachatryan *et al.* (CMS), *Phys. Rev. D* **93**, 032005 (2016), [Erratum: *Phys.Rev.D* **95**, 039906 (2017)], [arXiv:1509.03750 \[hep-ex\]](#).
- [123] A. M. Sirunyan *et al.* (CMS), *JHEP* **07**, 115 (2018), [arXiv:1806.03472 \[hep-ex\]](#).
- [124] A. Tumasyan *et al.* (CMS), *JHEP* **11**, 153 (2021), [arXiv:2107.13021 \[hep-ex\]](#).
- [125] C. Collaboration (CMS), (2022).
- [126] (2022), [arXiv:2212.12604 \[hep-ex\]](#).
- [127] A. Hayrapetyan *et al.* (CMS), (2023), [arXiv:2308.06143 \[hep-ex\]](#).
- [128] A. Hayrapetyan *et al.* (CMS), (2023), [arXiv:2307.08708 \[hep-ex\]](#).
- [129] G. Aad *et al.* (ATLAS), *Phys. Rev. Lett.* **127**, 141801 (2021), [arXiv:2105.13847 \[hep-ex\]](#).
- [130] M. Aaboud *et al.* (ATLAS), *JHEP* **07**, 117 (2019), [arXiv:1901.08144 \[hep-ex\]](#).
- [131] A. M. Sirunyan *et al.* (CMS), *Phys. Lett. B* **798**, 134992 (2019), [arXiv:1907.03152 \[hep-ex\]](#).
- [132] M. Abdullah, J. Calle, B. Dutta, A. Flórez, and D. Restrepo, *Phys. Rev. D* **98**, 055016 (2018), [arXiv:1805.01869 \[hep-ph\]](#).
- [133] M. Abdullah, M. Dalchenko, B. Dutta, R. Eusebi, P. Huang, T. Kamon, D. Rathjens, and A. Thompson, *Phys. Rev. D* **97**, 075035 (2018), [arXiv:1707.07016 \[hep-ph\]](#).
- [134] D. Barbosa, F. Díaz, L. Quintero, A. Flórez, M. Sanchez, A. Gurrola, E. Sheridan, and F. Romeo, *Eur. Phys. J. C* **83**, 413 (2023), [arXiv:2210.15813 \[hep-ph\]](#).
- [135] M. Abdullah, M. Dalchenko, T. Kamon, D. Rathjens, and A. Thompson, *Phys. Lett. B* **803**, 135326 (2020), [arXiv:1912.00102 \[hep-ph\]](#).
- [136] H. B. Nielsen and M. Ninomiya, *Nucl. Phys. B* **193**, 173 (1981).
- [137] H. B. Nielsen and M. Ninomiya, *Physics Letters B* **105**, 219 (1981).
- [138] S.-S. Xue, *Nucl. Phys. B* **486**, 282 (1997), [arXiv:hep-lat/9605005](#).
- [139] S.-S. Xue, *Nucl. Phys. B* **580**, 365 (2000), [arXiv:hep-lat/0002026](#).

- [140] S.-S. Xue, *Phys. Rev. D* **61**, 054502 (2000), [arXiv:hep-lat/9910013](#).
- [141] S.-S. Xue, *Phys. Lett. B* **737**, 172 (2014), [arXiv:1405.1867 \[hep-th\]](#).
- [142] S.-S. Xue, *Nucl. Phys. B* **990**, 116168 (2023), [arXiv:2210.04825 \[hep-ph\]](#).
- [143] W. A. Bardeen, C. T. Hill, and M. Lindner, *Phys. Rev. D* **41**, 1647 (1990).
- [144] S.-S. Xue, *Phys. Lett. B* **727**, 308 (2013), [arXiv:1308.6486 \[hep-ph\]](#).
- [145] I. Doršner, S. Fajfer, A. Greljo, J. F. Kamenik, and N. Košnik, *Phys. Rept.* **641**, 1 (2016), [arXiv:1603.04993 \[hep-ph\]](#).
- [146] I. Doršner and A. Greljo, *JHEP* **05**, 126 (2018), [arXiv:1801.07641 \[hep-ph\]](#).
- [147] I. Doršner, S. Fajfer, A. Greljo, J. F. Kamenik, and N. Košnik, *Phys. Rept.* **641**, 1 (2016), [arXiv:1603.04993 \[hep-ph\]](#).
- [148] L. Di Luzio and M. Nardecchia, *Eur. Phys. J. C* **77**, 536 (2017), [arXiv:1706.01868 \[hep-ph\]](#).
- [149] J. Alwall, M. Herquet, F. Maltoni, O. Mattelaer, and T. Stelzer, *JHEP* **06**, 128 (2011), [arXiv:1106.0522 \[hep-ph\]](#).
- [150] A. Alloul, N. D. Christensen, C. Degrande, C. Duhr, and B. Fuks, *Comput. Phys. Commun.* **185**, 2250 (2014), [arXiv:1310.1921 \[hep-ph\]](#).
- [151] C. Degrande, C. Duhr, B. Fuks, D. Grellscheid, O. Mattelaer, and T. Reiter, *Comput. Phys. Commun.* **183**, 1201 (2012), [arXiv:1108.2040 \[hep-ph\]](#).
- [152] T. Sjöstrand, S. Ask, J. R. Christiansen, R. Corke, N. Desai, P. Ilten, S. Mrenna, S. Prestel, C. O. Rasmussen, and P. Z. Skands, *Comput. Phys. Commun.* **191**, 159 (2015), [arXiv:1410.3012 \[hep-ph\]](#).
- [153] R. D. Ball et al. (NNPDF), *Eur. Phys. J. C* **77**, 663 (2017), [arXiv:1706.00428 \[hep-ph\]](#).
- [154] A. D. Martin, R. G. Roberts, W. J. Stirling, and R. S. Thorne, *Eur. Phys. J. C* **39**, 155 (2005), [arXiv:hep-ph/0411040](#).
- [155] V. Bertone, S. Carrazza, N. P. Hartland, and J. Rojo (NNPDF), *SciPost Phys.* **5**, 008 (2018), [arXiv:1712.07053 \[hep-ph\]](#).
- [156] M. L. Mangano, M. Moretti, F. Piccinini, and M. Treccani, *JHEP* **01**, 013 (2007), [arXiv:hep-ph/0611129](#).
- [157] “LQ UFO, https://cms-project-generators.web.cern.ch/cms-project-generators/LQ_UFO.tar.gz,” .
- [158] A. Tumasyan et al. (TOTEM, CMS), *Phys. Rev. Lett.* **129**, 011801 (2022), [arXiv:2110.05916 \[hep-ex\]](#).
- [159] P. Skands, S. Carrazza, and J. Rojo, *Eur. Phys. J. C* **74**, 3024 (2014), [arXiv:1404.5630 \[hep-ph\]](#).
- [160] J. de Favereau, C. Delaere, P. Demin, A. Giammanco, V. Lemaitre, A. Mertens, and M. Selvaggi (DELPHES 3), *JHEP* **02**, 057 (2014), [arXiv:1307.6346 \[hep-ex\]](#).
- [161] P. D. Group, (2021).
- [162] C. Collaboration, “Documentation of the RooStats-based statistics tools for Higgs PAG,” .
- [163] M. Aaboud et al. (ATLAS), *Eur. Phys. J. C* **79**, 803 (2019), [arXiv:1906.03204 \[hep-ex\]](#).
- [164] M. Aaboud et al. (ATLAS), *Eur. Phys. J. C* **78**, 102 (2018), [arXiv:1709.10440 \[hep-ex\]](#).
- [165] A. M. Sirunyan et al. (CMS), *JHEP* **04**, 114 (2019), [arXiv:1812.10443 \[hep-ex\]](#).
- [166] A. M. Sirunyan et al. (CMS), *JHEP* **05**, 052 (2020), [arXiv:2001.04521 \[hep-ex\]](#).

- [167] A. Tumasyan et al. (CMS), *Phys. Lett. B* **843**, 137803 (2023), [arXiv:2210.03082 \[hep-ex\]](#).
- [168] A. M. Sirunyan et al. (CMS), *JHEP* **04**, 015 (2019), [arXiv:1811.03052 \[hep-ex\]](#).
- [169] V. Khachatryan et al. (CMS), *JHEP* **03**, 125 (2016), [arXiv:1511.01407 \[hep-ex\]](#).